Heliyon

ELSEVIER

Received:
23 December 2018
Revised:
13 March 2019
Accepted:
1 April 2019

Cite as: A. Pramanik, A. K. Basak, C. Prakash. Understanding the wire electrical discharge machining of Ti6Al4V alloy. Heliyon 5 (2019) e01473. doi: 10.1016/j.heliyon.2019.e01473

Understanding the wire electrical discharge machining of Ti6Al4V alloy

A. Pramanik [a,*], **A. K. Basak** [b], **C. Prakash** [c]

[a] *School of Civil and Mechanical Engineering, Curtin University, Bentley, WA, Australia*

[b] *Adelaide Microscopy, University of Adelaide, Adelaide, SA, Australia*

[c] *School of Mechanical Engineering, Lovely Professional University, Phagwara, Punjab 144411, India*

[*] Corresponding author.

E-mail address: alokesh.pramanik@curtin.edu.au (A. Pramanik).

Abstract

Non-conventional machining process for instance, wire electrical discharge machining (WEDM) of titanium alloys is gaining attention due to non-contact nature of this process. To deepen the understanding in this area, this study investigates surface generation, kerf width, discharge gap, material removal rate and wire degradation during WEDM of Ti6Al4V alloy. Pulse on time (4−10 μs), flushing pressure (7−18 MPa) and wire tension (800−1700 gf) were varied and resulting influences on output parameters were analysed. It was found that, machined surfaces consist of multi-layered recast layer with the presence of cracks, holes as well as traces of materials from electrode wire. The composition and roughness of the machined surface varies slightly with respect to machining condition without following any trend. In addition, deformation and morphology of deformed wire electrode after the WEDM process was also reported in this study.

Keyword: Mechanical engineering

1. Introduction

Ti6Al4V is one of the most popular alloys in titanium alloys family which is predominantly used in many advanced applications such as aerospace and biomedical

https://doi.org/10.1016/j.heliyon.2019.e01473

industries [1]. There are number of challenges towards machining/processing of this alloy because of its lower thermal conductivity, greater strength and chemically reactiveness. As a results, high cutting tool wear, lower material removal rate (MRR), higher machining forces, tool vibration and worse surface finish are almost inevitable [2, 3, 4]. To avoid these aforementioned complexities during tradition machining, no-traditional machining such as WEDM is a common alternative towards the machining of titanium alloys. During WEDM, the workpiece is sunken in dielectric fluid to generate a favourable surrounding for electric spark formation to take place [5, 6, 7]. During the process, spark erosion occurs in the neighbourhood of electrodes and form anticipated two/three dimensional shapes based on input process variables by melting/evaporating the workpiece [8, 9]. The difference between WEDM and conventional EDM is the use of thin wire electrode (Ø 0.05−0.3 mm) in the former case. The wire act as an electrode and moves uninterruptedly maintaining a discharge gap with the workpiece. Electric pulses of high frequency pass through the space between the wire electrode and workpiece, and discharge sparks. The material removal occurs by this spark discharges ahead of the moving wire electrode [5, 10, 11, 12].

A number of reports are available in literatures on the influence of WEDM variables on MRR during the process. Prasad *et al.* [13] concludes that, a rise in MRR as well as peak current takes place with the rise of pulse on time. Kumar *et al* found the rise of wire tension and pulse on time increases the wire breakage frequency during WEDM of pure titanium [14]. Sivaprakasam *et al.* conducted an experimental investigation on influence of capacitance, feed rate and voltage on surface finish, kerf width and MRR during micro-WEDM of Ti6Al4V alloy and reported that MRR rises with the rise of electric voltage [15]. Low flushing pressure induce spark gap pollution which caused a sudden decrease in MRR during increased discharge energy. Optimum value was achieved at 10 nF capacitance as smaller kerf width, least machining time and smoother surface was prominent. During WEDM of grade 5 titanium alloy by a diffused brass (37 wt. % Zinc and 63 wt. % Copper) wire electrode, Arikatla *et al.* noted that, an increase of wire feed, pulse on time, server voltage, wire tension and input power increases the kerf width where the significant contribution was from pulse on time, input power and sever voltage [16]. In addition, inverse relationship existed between feed rate and kerf width. Aniza *et al.* also noted a decrease in kerf width with increase feed rate [17]. Therefore, it was suggested to avoid higher feed rate to achieve accurate kerf width. Aspinwall *et al.* observed that, short duration and high frequency pulse contributed towards lower workpiece damages during WEDM of Ti6Al4V alloy where the recast layer thickness was minimum [18]. M. Manjaiah *et al.* observed that, an increased discharge current resulted in increased surface roughness due to increased spark strike rate on its surface [19]. Surface finish is more favourable, if the pulse off time is longer at certain discharge current. Kumar *et al.* investigated the influence of peak current, pulse on/off time and spark gap

https://doi.org/10.1016/j.heliyon.2019.e01473

voltage on the finish of the surface of pure titanium during WEDM by brass wire electrode [20]. According to their findings, higher pulse on time and peak current form wider and deeper irregular topography and poor surface quality; whereas, better surface texture occurred at lower values of electrical process parameters. Lenin *et al.* concluded that, kerf width rises with the rise of pulse on time as well [21]. Further, taper occurs towards the completion of machining. The cutting width tends to be greater in comparison of electrode wire width. Average kerf width of 0.335 mm by brass wire electrode was best based on machining cost and time [22]. Alias et al. reported that, increase of pulse off time from 1 to 5 μs and peak current from 4 to 12 A increase the kerf width significantly [23]. Nevertheless, the contribution of pulse off time was higher that of peak current. The optimum arrangement of cutting variables for kerf width were peak current of 12 A, pulse on time of 5 μs, wire speed of 4 mm/min and wire tension of 6 N.

The above discussion indicates that, there are many investigations on WEDM of titanium alloys. However, the ranges and variation of parameters considered in those investigations are very limited, representing a narrow range. In addition, further details on machined surface, kerf width, spark gap and tool electrode wire are required to better understand the WEDM of titanium alloy for widening it applications. To address these issues, this study varies wire tension, flushing pressure and pulse on time in a wider range and examine the influence of these variables on machined surface, kerf width, spark gap, MRR and degradation of wire electrode.

2. Materials & methods

Ti6Al4V alloy was machined using the FANUC ROBOCUT ∝ 0iD WEDM. Table 1 shows the chemical compositions of Ti6Al4V alloy. Cylindrical blocks of Ø 12 mm were machined from 9 mm thick titanium plates at different machining conditions as shown in Table 2. Brass wire of Ø 0.25 mm coated with zinc was used as tool electrode during all the experiments under 10 l/min flushing rate, 85 V open circuit voltage, 10 m/min wire speed, 20 V servo voltage, and 26 μs pulse off time. Deionized water was used as di-electric fluid. The surfaces of Ti6Al4V and wire after machining were investigated by energy dispersive x-ray (EDX) equipped field emission scanning electron microscope (Quanta 450 FE-SEM, FEI).

Mitutoyo Surtest SJ-201 with 0.0025 mm radius stylus tip was used to measure the roughness of the machined surfaces using a cut off length of 0.8 mm. The stylus of

Table 1. Elements in Ti-6Al-4V alloy as analysed by EDX.

Elements	Sn	C	Mn	Si	Cr	Fe	V	Al	Ti
Composition (wt. %)	0.001	0.006	0.0053	0.01	0.021	0.091	3.714	6.321	89.83

https://doi.org/10.1016/j.heliyon.2019.e01473

Table 2. Design of experiments.

Expt. no.	Pulse on time (μs)	Flushing pressure (MPa)	Wire Tension (gf)
1	4	15	1400
2	6	15	1400
3	8	15	1400
4	10	15	1400
5	8	10	1400
6	8	7	1400
7	8	18	1400
8	8	15	1100
9	8	15	800
10	8	15	1700

the tester was placed at a chosen position and then gently dragged automatically across the surface. Then the measured arithmetic surface roughness (Ra) was digitally displayed in the instrument. The kerf width was measured by Olympus BX51M optical microscope at 50x magnification which was used to calculate the material removal rate. The spark gap was calculated by halving the deductions of wire diameter from average kerf width.

3. Results and discussion

3.1. Machined surface

Fig. 1 presents the elemental composition (wt. %) and morphology of machined surface of titanium alloy generated from WEDM at different pulse; where the flushing pressure and wire tension were constant at 15 MPa and 1400 gf, respectively. The machined surfaces contain multi-layered recast layer, as show in the cross-section images in Fig. 2. The inner layer looks solid with lots of cracks and holes in it, whereas the outer layers are discontinuous flaky type islands on the top of solid layer. The localised flaky layers don't contain any cracks in it. The population of the flakes varies with the pulse on time, as the flakes rises with the rise of pulse on time till 8 μs (Fig. 1c). At 8 μs of pulse on time, flakes are so densely populated that the cracks on solid layer are not clearly visible. After that, the flakes are merged/strongly bonded with the layer underneath at 10 μs of pulse on time and the visibility of the cracks increase as shown in Fig. 1 (d). The machined surface also experienced the diffusion of elements such as, Zn and Cu from electrode wire. The amount of diffusion varies with the variation of pulse on time, but no specific trend was noticed between pulse on time and elemental diffusion.

Fig. 3 shows the composition (wt. %) and morphology of machined titanium alloy surface by WEDM at different flushing pressure when the pulse on time and wire

https://doi.org/10.1016/j.heliyon.2019.e01473

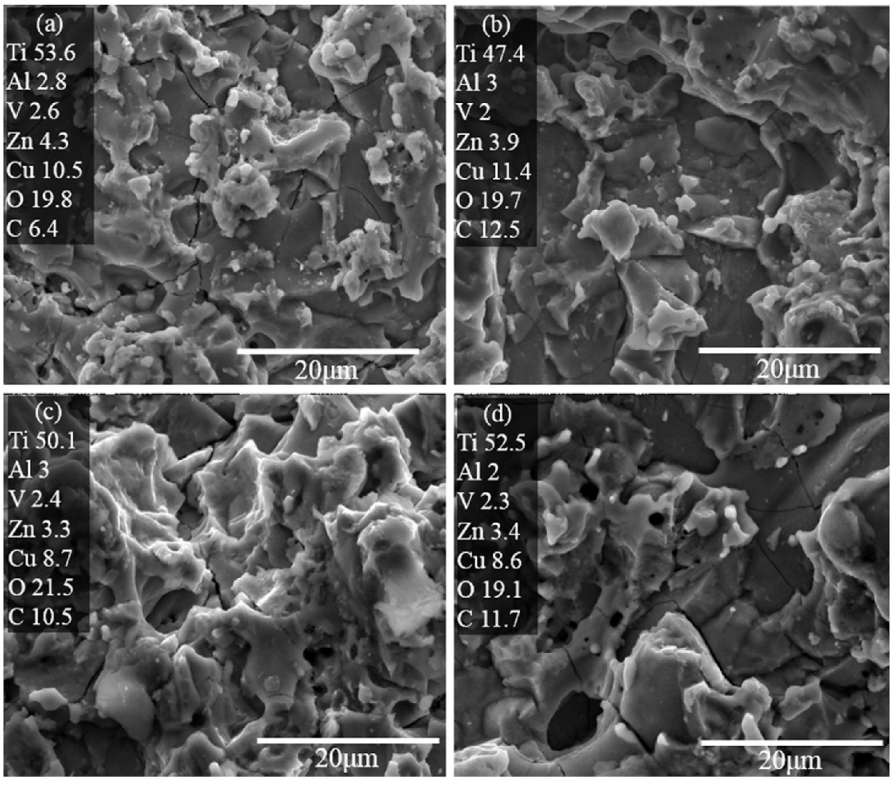

Fig. 1. Composition (wt. %) and morphology of machined surface of titanium alloy after WEDM at different pulse on time: (a) 4, (b) 6, (c) 8 and (d) 10 μs; when the flushing pressure and wire tension were 15 MPa and 1400 gf, respectively.

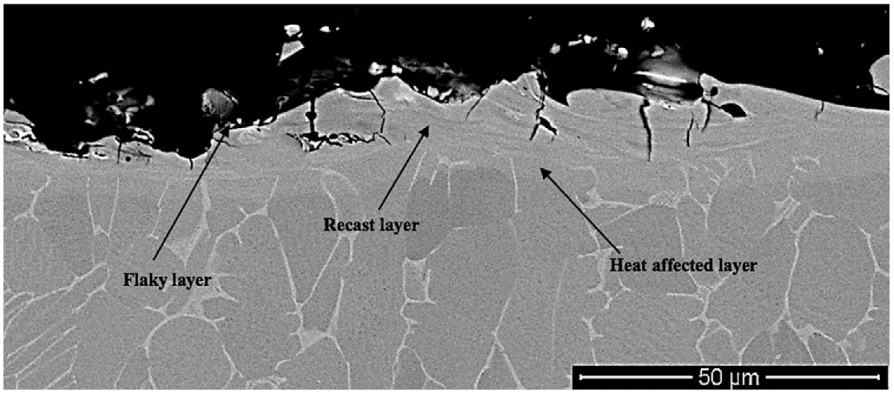

Fig. 2. Typical cross-sectional view of Ti6Al4V surface machined by wire EDM.

tension were constant at 8 μs and 1400 gf, respectively. In this case, flaky layers were connected to each other and, the cracks and holes are visible on it. The underneath solid layer can be seen through the holes of flaky layers where it is discontinuous. No significant difference in the surface appearance was noticed with the variation of flushing pressure except at 15 MPa (Fig. 3 c) where the flaks are highly populated and appear loosely connected with solid underneath layer compared to the other

https://doi.org/10.1016/j.heliyon.2019.e01473

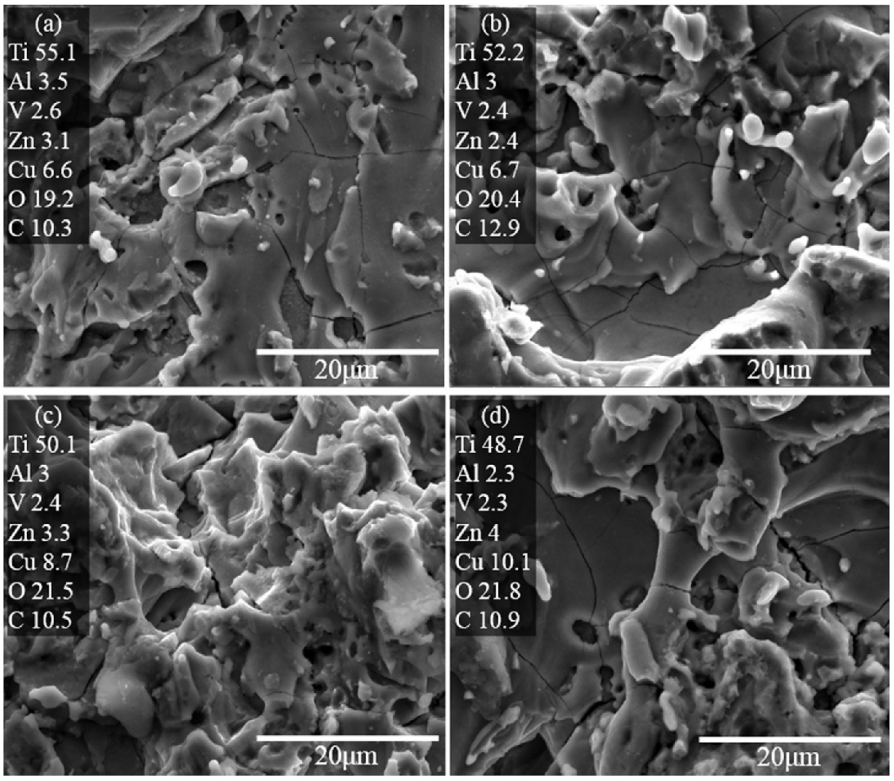

Fig. 3. Composition (wt. %) and morphology of machined surface of titanium alloy after WEDM at different flushing pressure: (a) 7, (b) 10, (c) 15 and (d) 18 MPa when the wire tension and pulse on time are of 1400 gf and 8 μs, respectively.

cases. The amount of wire electrode material diffusion also affected by the variation of flushing pressure. The maximum amount of diffusion of Zn and Cu were noticed at highest flushing pressure of 18 MPa (Fig. 3d).

It seems that, the cooling rate of the outer surface does not vary significantly with the variation of flushing pressure of electrolyte after machining. Therefore, the appearance of machined surface doesn't vary noticeably. It is not known yet why the flaks are highly populated and appear loosely connected with solid underneath layer at 15 MPa flushing pressure. However, this might be because of the discrete nature of EDM where the spark gap is not even at all times [24, 25, 26, 27, 28, 29, 30, 31].

Fig. 4 demonstrates the composition (wt. %) and morphology of machined titanium alloy surface produced by WEDM at different wire tension when the flushing pressure and pulse on time ere 15 MPa and 8 μs, respectively. In this case, the flaky layers are connected to each other but distributed non-uniformly and the occurrence of visible cracks and holes are much less prominent compared to those shown in Fig. 4. The solid underneath layer can be seen through the holes of flaky layers where it is discontinuous. The number of flakes increase and become more solidified and uniform while the wire tension rises. The number of visible cracks is much less

https://doi.org/10.1016/j.heliyon.2019.e01473

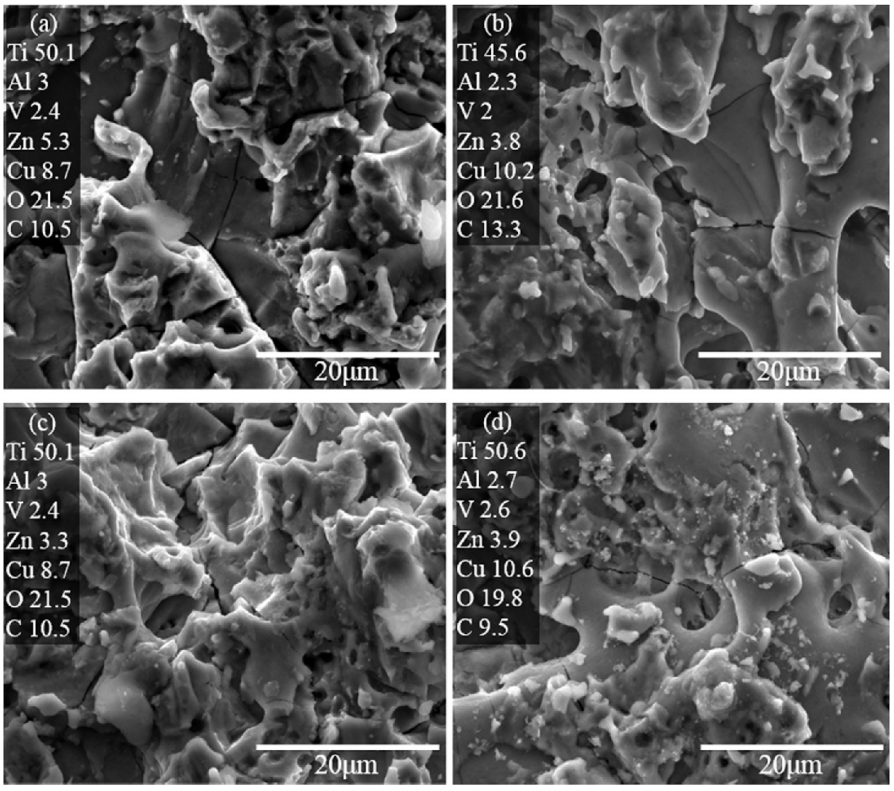

Fig. 4. Composition (wt. %) and morphology of machined surface of titanium alloy after WEDM at different wire tension: (a) 800, (b) 1100, (c) 1400 and (d) 1700 gf when the pulse on time and flushing pressure were of 8 μs and 15 MPa, respectively.

compare to Fig. 3 and remains unchanged with the variation of tension in wire. The amount of wire electrode material diffusion also affected by the variation of the flushing pressure. However, no specific trend was noticed between the amount of element diffusion and wire tension.

The tension in wire controls its flexibility and became relatively rigid at higher wire tension. A longer length of wire takes part in machining when the wire tension is low where the wire has more chance to vibrate and deviate from the expected travel path. Thus, it might remove flakes around the machining zones and induces a non-uniform appearance due to flexible nature of the wire electrode. Therefore, all these might be minimised with the rigid wire at higher tension.

In all cases, as mentioned above, it is interesting to note that, multilayered recast layers form on titanium alloy surface generated by WEDM. This kind of recast layer must be occurring due to the distinguished properties of titanium alloy such as, chemical reactivity at high temperature, high melting point, low thermal conductivity and low density. It seems that, the flaky layer is made of mostly oxides, as confirmed by EDX analysis, due to oxidation as a result of electrolysis of the electrolyte. The flaky appearance took place due to rapid cooling of the molten/semi-

https://doi.org/10.1016/j.heliyon.2019.e01473

molten material. The underneath solid layer just below the flaky layer is formed when the Ti6Al4V is cooled under very high rate cooling rate. Ti6Al4V alloy has very low thermal conductivity, and therefore cooling rate vary significantly from layer to layer of the workpiece. The outermost surface experience highest temperature and cooling rate and subsequent decrease of heat transfer along the depth of the workpiece contribute to form the recast layer in multiple layers.

The influence of input parameters on the machined surfaces roughness are shown in Fig. 5. The disparity of surfaces roughness is not significant and there is no noticeable trend of surface roughness while varying flushing pressure and wire tension. This is highly expected, as the flushing pressure and wire tension don't contribute to electric discharge directly; however, help to clean the machining zone and sustain the accuracy of machining respectively. Material is removed by a series of electrical sparks that rise the temperature in the range of 8000−12000 °C between the workpiece and the electrode [29]. WEDM is a discrete process, where the machining environment varies time to time depending on local temperature build-up, concentration and size of debris, wire electrode deformation and wear etc [30]. Therefore, very irregular surfaces are generated as shown in Figs. 1, 3, and 4. The irregular distribution of cracks and flakes of different sizes on machined surface don't allow to have any specific trend for the rage of flushing pressure and wire tension considered in this investigation. On the other hand, as shown in Fig. 5, shorter pulse on times (4 and 6 μs) offer lower surface roughness compares to that of longer pulse on times (8 and 10 μs). This is well know that, shorter pulse on time generates less discharge energy at a time which produces shallower crater and provides smoother ups and downs on the machined surfaces and results comparatively lower surface roughness [5].

3.2. Kerf width and spark gap

The kerf width is the real gap across the slot after machining, which is generally larger than the diameter of wire electrode. The kerf widths at top and bottom of

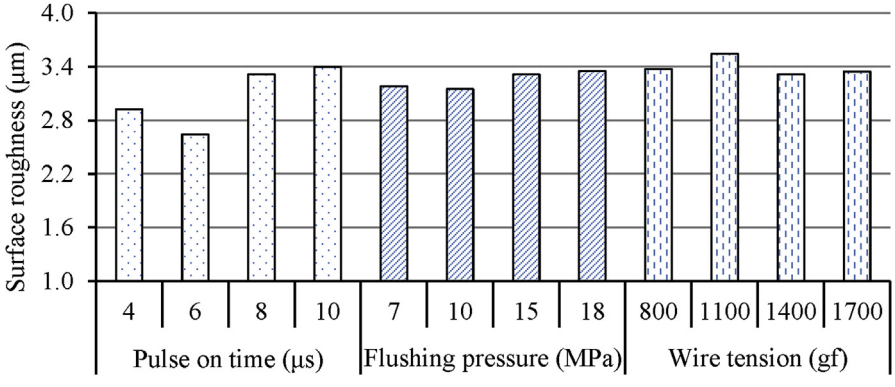

Fig. 5. Effect of variation of (a) pulse on time, (b) flushing pressure and (c) wire tension on surface roughness of machined surface of titanium alloy after WEDM.

https://doi.org/10.1016/j.heliyon.2019.e01473

the workpieces generally vary because of the wear or deformation of electrode wire and change of electrolyte concentration. Fig. 6 shows the influence of pulse on time (Fig. 6a), flushing pressure (Fig. 6b) and wire tension (Fig. 6c) on the width of kerf at top and bottom of the workpiece during WEDM of Ti6Al4V alloy. The kerf widths at the bottom and top of the slot are seen to increase with the rise of pulse on time. This is because of dissipation of more energy at a time with the rise of pulse on time. The variation between top and bottom kerf widths is insignificant as pulse on time varies. This might be due to the balancing out of the wire electrode deformation with the change of properties of electrolyte due to debris formation (oxide) during machining.

The top kerf width is much higher than that at bottom at lower flushing pressure. This is due to the contamination of electrolyte at low pressure due to the formation debris which changes the electrical properties of dielectric and reduces the efficiency of material removal. This reduces the kerf width at the bottom. In addition, fresh unwearied wire electrode generates bigger kerf at the top. The smaller kerf with at the bottom is because of wear of wire electrode. With the rise of flushing pressure, the dissimilarity between the top and bottom kerf widths decreases through balancing wire electrode deformation and wear, and electrical properties of electrolyte. Both the top and bottom kerf widths increase significantly with further increase of flushing pressure which might be due to better cooling of the wire electrode which reduces wear and deformation, and cleaned spark zone at high flushing pressure.

The widths of kerf at the bottom and top are seen to decrease with the rise of tension in wire as shown in Fig. 6c. As previously mentioned, tension in wire influences the flexibility of electrode wire. At lesser tension, the wire remains stretchy and active length of wire is longer which induces more heat and removes more materials; thus, produces wider kerf. On the other hand under higher tension, the wire electrode becomes rigid and the diameter of the wire decreases which gives reduced kerf width. The variance between the bottom and top kerf widths does not follow any trend.

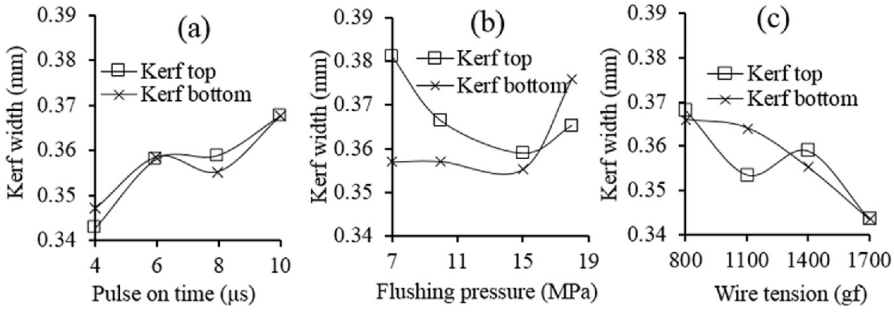

Fig. 6. Effect of (a) pulse on time, (a) flushing pressure and (c) wire tension on kerf width during WEDM of titanium alloy.

https://doi.org/10.1016/j.heliyon.2019.e01473

Similar to kerf width, spark gap also varies with machining parameters as well as wire electrode diameter and properties of electrode. The influence of flushing pressure, wire tension and pulse on time on average spark gap is presented in Fig. 7. The average trends, as seen in the graphs, spark gaps increase with the rise of pulse on time but decreases with the rise of wire tension and flushing pressure. Increased pulse on time induces more energy at a time and removes more materials which creates increase spark gap. The higher flushing pressure cleans the debris from machining zone more efficiently and reduces the chance for debris to concentrate which leads to reduced spark gap. On the other hand, the wire becomes rigid at higher tension and the wire diameter decreases which gives reduced spark gap. It is unexpected that the spark gap at 4 μs of pulse on time and 1400 of gf wire tension is higher than that at 6 μs of pulse on time and 1100 of gf wire tension as displayed in Fig. 7. The reason of these are not known yet withstanding the fact that, EDM is a discrete process and thus the spark gap is not even at all times. This strange results might be due to the frenzied spark, disparity of electrolyte properties and flush rate because of blocking by debris [31].

3.3. Material removal rate

The pule-on-time contributes towards the heat input, flushing pressure affect the removal of debris and replacement of fresh dielectric, and the wire tension contributes towards the flexibility of the wire i.e. the mechanical capability to continue the procedure steadily [25]. The influence of pulse on time, flushing pressure and tension in wire on MRR is presented in Fig. 8. The average trends is that, MRR increase with the rise of pulse on time but it decreases with the rise of wire tension. The reasons for increased MRR with the rise of pulse on time and decreased tension in wire are already explained above. Fig. 8 also indicates that MRR at low flushing pressure (7 MPa) is comparatively low but with the rise of flushing pressure, MRR increases and then it remains almost constant with further increase of flushing pressure. It seems that, at low flushing pressure the debris clogs the machining zone and sparks

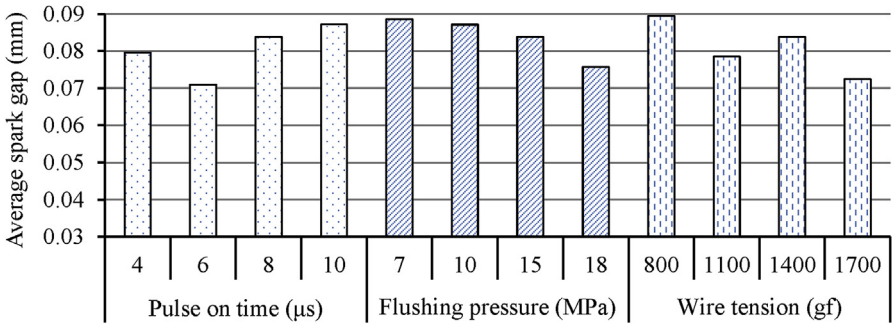

Fig. 7. Influence of variation of (a) pulse on time, (b) flushing pressure and (c) wire tension on average spark gap during WEDM of titanium alloy.

https://doi.org/10.1016/j.heliyon.2019.e01473

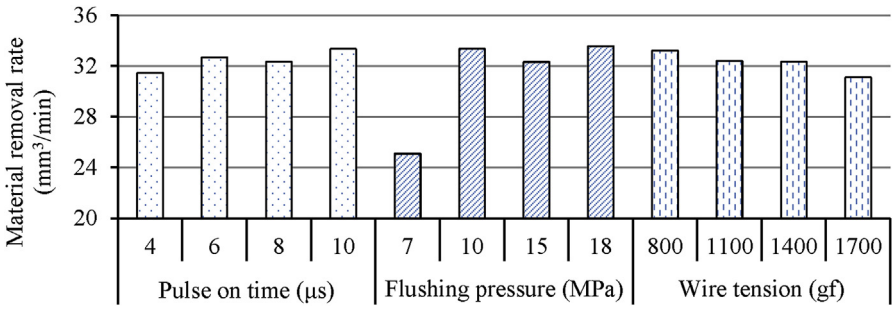

Fig. 8. Effect of variation of (a) pulse on time, (b) flushing pressure and (c) wire tension on MRR during WEDM of titanium alloy.

happen without removing any materials. On the other hand, a balanced machining environment is maintained at higher flushing pressure which leads almost steady material removal rate.

3.4. Wire degradation

During WEDM process, wire material is also removed gradually in addition to workpiece material due to generation of high temperature. The wire electrode also experience significant deformation due to high temperature and tension, and in many instances the wire fails (physically brake down) during machining process [12,32]. Fig. 9 represent the fresh and unused wire surface and its composition. Uniformly oriented Zn grains are visible on the surface as confirmed by EDX analysis. However, the morphology of the wires changes completely after using it in the machining process. The influences of pulse on time, flushing pressure and tension in wire on the composition and morphology of used unbroken wire electrode are given in Figs. 10, 11 and 12. The figures confirm, the depletion of Zn coating from the surface of the wire as well as spreading of melted Cu from wire core. The EDX results indicate that the used wire surface mostly consists of Zn and Cu though the traces of Ti, Al and V were also noticed; which was transferred from

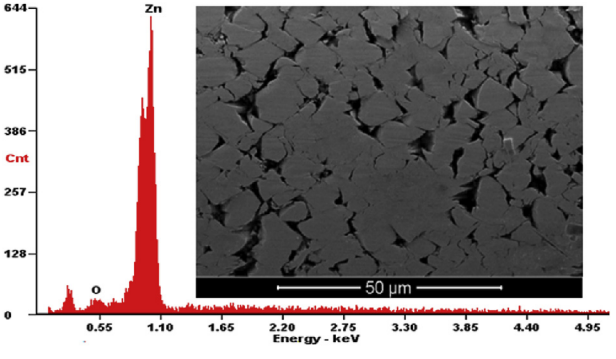

Fig. 9. Morphology and composition of unused wire electrode.

https://doi.org/10.1016/j.heliyon.2019.e01473

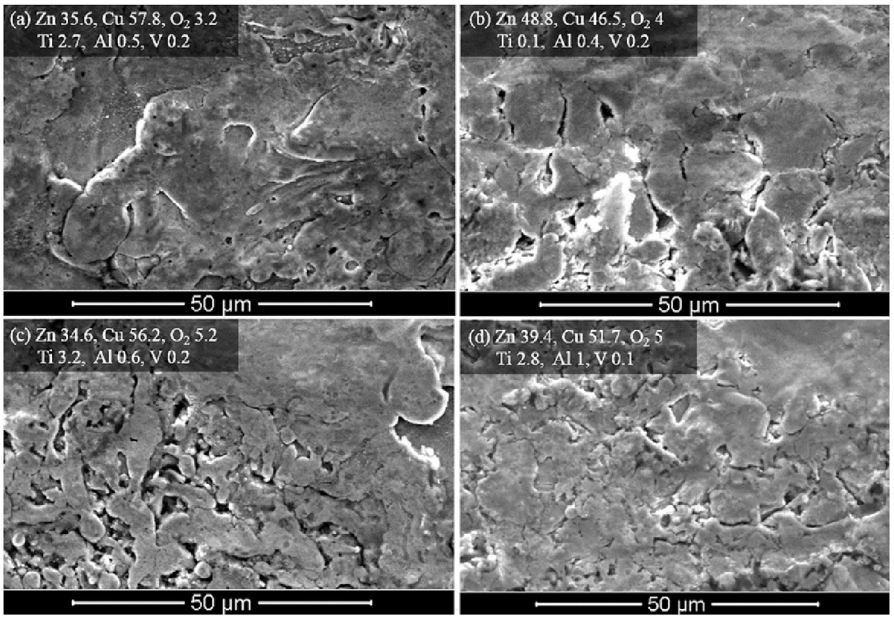

Fig. 10. Morphology and composition of wire electrode after WEDM of titanium alloy at different pulse on time: (a) 4, (b) 6, (c) 8 and (d) 10 μs under flushing pressure and wire tension of 15 MPa and 1400 gf, respectively.

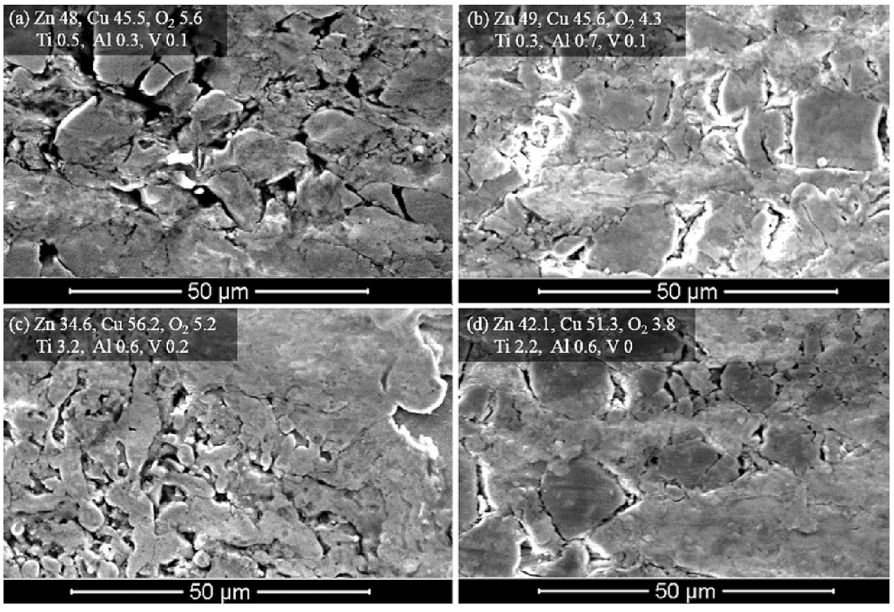

Fig. 11. Morphology and composition of wire electrode after WEDM of titanium alloy at different flushing pressure: (a) 7, (b) 10, (c) 15 and (d) 18 MPa under pulse on time and wire tension of 8 μs and 1400 gf, respectively.

workpiece material due to spattering and diffusion. There were no noticeable variation of wire morphology with the variation of input parameter. However, minor change of composition was noticed with the variation of input parameters which

https://doi.org/10.1016/j.heliyon.2019.e01473

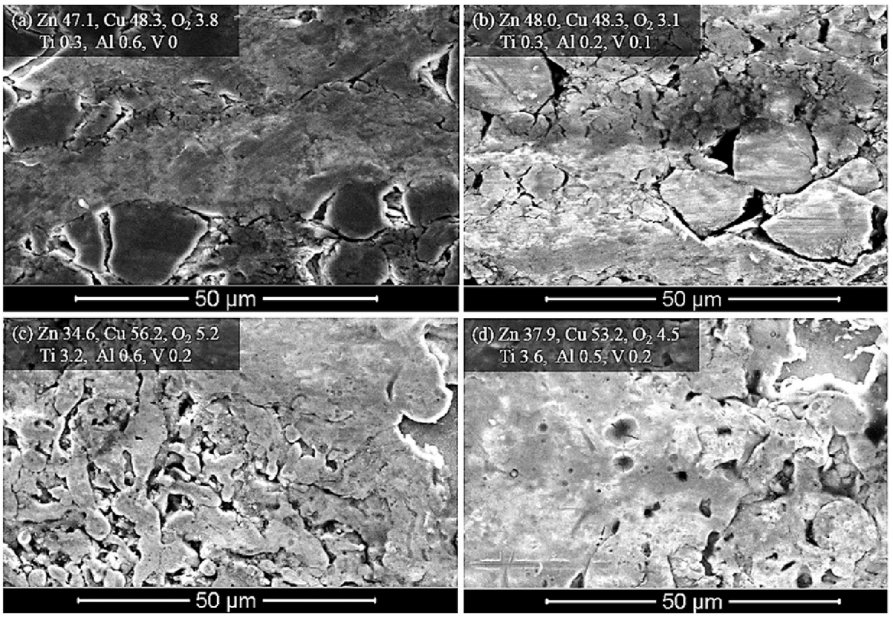

Fig. 12. Morphology and composition of wire electrode after WEDM of titanium alloy at different wire tension: (a) 800, (b) 1100, (c) 1400 and (d) 1700 gf under pulse on time and flushing pressure of 8 μs and 1400 MPa, respectively.

didn't follow any trend. The events of electric spark are non-uniform and inconsistent, which result in irregular existence of workpiece material on electrode wire.

The adhesion of molten/semi-molten workpiece material on wire electrode usually takes place during sparking because of spattering [25]. The used wire surface displays existence of a number of craters because of spark and re-deposition of frozen workpiece material.

4. Conclusions

The present research examines the influence of wide range of machining variables such as, pulse on time (4−10 μs), flushing pressure (7−18 MPa) and wire tension (800−1700 gf) on the morphology of machined surfaces during WEDM of Ti6Al4V alloy. In addition to machined surface morphology for example, recast layer formation and surface roughness, kerf width, discharge gap, material removal rate and degradation of wire electrode was also analysed pertaining to input variables. Based on the experimental data and aforementioned data analyses/discussion, following conclusions can be drawn:

(a) The machined surfaces consist of multi-layered recast layer with the presence of cracks, holes as well as traces of wire electrode materials. The top layer of the recast layer is mostly the flaky spattered oxides which is discontinuous in nature and weakly attached with underneath solid layer. The population of

https://doi.org/10.1016/j.heliyon.2019.e01473

the flaks varies with machining conditions. The underneath of recast layer is solid and dense.

(b) The variation of surface morphology and composition of the machined surface with respect to machining conditions is not significant. The slight variations of these output parameters with machining conditions don't follow any trend. Shorter pulse on times (4 and 6 μs) gave lower surface roughness. There is no noticeable variation and trend of surface roughness while varying flushing pressure and wire tension.

(c) The kerf widths at the bottom and top of the slot are seen to increase with the rise of pulse on time. The kerf width at the top is much higher than that at bottom at low flushing pressure. The kerf widths at the bottom and top are seen to decline with the rise of tension in wire. In general, MRR increases with the rise of pulse on time, and decreases with the increase of tension in wire; but with the increase of flushing pressure, MRR initially increases and then remains almost unchanged.

(d) During WEDM process, Zn coating on the wire electrode became depleted and wears out in addition to splashing of melted Cu from wire core. The influence of input parameters on wire morphology and composition is negligible. The wire surface also contains traces of workpiece material which might transfer due to spattering and diffusion.

Declarations

Author contribution statement

Alokesh Pramanik: Conceived and designed the experiments; Performed the experiments; Analyzed and interpreted the data; Contributed reagents, materials, analysis tools or data; Wrote the paper.

Animesh Basak: Performed the experiments; Analyzed and interpreted the data; Contributed reagents, materials, analysis tools or data; Wrote the paper.

Chander Prakash: Analyzed and interpreted the data; Wrote the paper.

Funding statement

This research did not receive any specific grant from funding agencies in the public, commercial, or not-for-profit sectors.

Competing interest statement

The authors declare no conflict of interest.

https://doi.org/10.1016/j.heliyon.2019.e01473

Additional information

No additional information is available for this paper.

References

[1] A. Pramanik, G. Littlefair, Developments in machining of stacked materials made of CFRP and titanium/aluminum alloys, Mach. Sci. Technol. 18 (4) (2014) 485−508.

[2] A. Pramanik, G. Littlefair, Machining of titanium alloy (Ti-6Al-4V)—theory to application, Mach. Sci. Technol. 19 (1) (2015) 1−49.

[3] A. Pramanik, Problems and solutions in machining of titanium alloys, Int. J. Adv. Manuf. Technol. 70 (5−8) (2014) 919−928.

[4] Machining and tool wear mechanisms during machining titanium alloys, in: A. Pramanik, M. Islam, A. Basak, G. Littlefair (Eds.), Advanced Materials Research, Trans Tech Publ, 2013.

[5] A. Pramanik, A. Basak, A. Dixit, S. Chattopadhyaya, Processing of duplex stainless steel by WEDM, Mater. Manuf. Process. (2018) 1−9.

[6] A. Pramanik, G. Littlefair, Wire EDM mechanism of MMCs with the variation of reinforced particle size, Mater. Manuf. Process. 31 (13) (2016) 1700−1708.

[7] A. Pramanik, M.N. Islam, B. Boswell, A.K. Basak, Y. Dong, G. Littlefair, Accuracy and finish during wire electric discharge machining of metal matrix composites for different reinforcement size and machining conditions, Proc. IME B J. Eng. Manufact. 232 (6) (2018) 1068−1078.

[8] A. Kumar, A. Mandal, A.R. Dixit, A.K. Das, Performance evaluation of Al2O3 nano powder mixed dielectric for electric discharge machining of Inconel 825, Mater. Manuf. Process. 33 (9) (2018) 986−995.

[9] J.C. Pilligrin, P. Asokan, J. Jerald, G. Kanagaraj, Effects of electrode materials on performance measures of electrical discharge micro-machining, Mater. Manuf. Process. 33 (6) (2018) 606−615.

[10] E.K. Mussada, C.C. Hua, A.K.P. Rao, Surface hardenability studies of the die steel machined by WEDM, Mater. Manuf. Process. (2018) 1−6.

[11] S. Kar, P.K. Patowari, Electrode wear phenomenon and its compensation in micro electrical discharge milling: a review, Mater. Manuf. Process. (2018) 1−27.

 https://doi.org/10.1016/j.heliyon.2019.e01473

[12] A. Pramanik, A. Basak, Sustainability in wire electrical discharge machining of titanium alloy: understanding wire rupture, J. Clean. Prod. 198 (2018) 472–479.

[13] A.R. Prasad, K. Ramji, G. Datta, An experimental study of wire EDM on Ti-6Al-4V Alloy, Proc. Mater. Sci. 5 (2014) 2567–2576.

[14] A. Kumar, V. Kumar, J. Kumar, Investigation of machining parameters and surface integrity in wire electric discharge machining of pure titanium, Proc. IME B J. Eng. Manufact. 227 (7) (2013) 972–992.

[15] P. Sivaprakasam, P. Hariharan, S. Gowri, Modeling and analysis of micro-WEDM process of titanium alloy (Ti–6Al–4V) using response surface approach, Eng. Sci. Technol. Int. J. 17 (4) (2014) 227–235.

[16] S.P. Arikatla, K.T. Mannan, A. Krishnaiah, Parametric optimization in wire electrical discharge machining of titanium alloy using response surface methodology, Mater. Today Proc. 4 (2) (2017) 1434–1441.

[17] Influence of machine feed rate in WEDM of titanium Ti-6Al-4V with constant current (6A) using brass wire, in: A. Aniza, A. Bulan, M.A. Norliana (Eds.), Int. Symp on Robotics and Intelligent Sensors, 2012.

[18] D. Aspinwall, S. Soo, A. Berrisford, G. Walder, Workpiece surface roughness and integrity after WEDM of Ti–6Al–4V and Inconel 718 using minimum damage generator technology, CIRP Ann. Manuf. Technol. 57 (1) (2008) 187–190.

[19] M. Manjaiah, S. Narendranath, S. Basavarajappa, V. Gaitonde, Wire electric discharge machining characteristics of titanium nickel shape memory alloy, Trans. Nonferrous Metals Soc. China 24 (10) (2014) 3201–3209.

[20] A. Kumar, V. Kumar, J. Kumar, Parametric effect on wire breakage frequency and surface topography in WEDM of pure titanium, J. Mech. Eng. Technol. 1 (2) (2013) 51–56.

[21] S.D. Lenin, A. Uthirapathi, R.R.P.S. Venkata, M. Durai Selvam, Influence of pulse-on-time on the performance of wire electrical discharge machining of Ti-6Al-4V using zinc coated brass wire, Appl. Mech. Mater. 592–594 (2014) 416–420.

[22] M.K. Kuttuboina, A. Uthirapathi, S.D. Lenin, Effect of process parameters in electric discharge machining of Ti-6Al–4V alloy by three different tool electrode materials, Adv. Mater. Res. 488–489 (2012) 876–880.

 https://doi.org/10.1016/j.heliyon.2019.e01473

[23] A. Alias, B. Abdullah, N.M. Abbas, Influence of machine feed rate in WEDM of titanium Ti-6Al-4V with constant current (6A) using brass wire, Proc. Eng. 41 (2012) 1806–1811.

[24] A. Pramanik, A. Basak, M.N. Islam, G. Littlefair, Electrical discharge machining of 6061 aluminium alloy, Trans. Nonferrous Metals Soc. China 25 (9) (2015) 2866–2874.

[25] A. Pramanik, Electrical discharge machining of MMCs reinforced with very small particles, Mater. Manuf. Process. 31 (4) (2016) 397–404.

[26] A. Mohanty, G. Talla, S. Gangopadhyay, Experimental investigation and analysis of EDM characteristics of Inconel 825, Mater. Manuf. Process. 29 (5) (2014) 540–549.

[27] L. Li, Z. Li, X. Wei, X. Cheng, Machining characteristics of Inconel 718 by sinking-EDM and wire-EDM, Mater. Manuf. Process. 30 (8) (2015) 968–973.

[28] T. Ahmed, H. Rack, Phase transformations during cooling in $\alpha+\beta$ titanium alloys, Mater. Sci. Eng. 243 (1-2) (1998) 206–211.

[29] S. Abdulkareem, A. Ali Khan, M. Konneh, Cooling effect on electrode and process parameters in EDM, Mater. Manuf. Process. 25 (6) (2010) 462–466.

[30] V. Srivastava, P.M. Pandey, Performance evaluation of electrical discharge machining (EDM) process using cryogenically cooled electrode, Mater. Manuf. Process. 27 (6) (2012) 683–688.

[31] P. Saha, D. Tarafdar, S.K. Pal, P. Saha, A.K. Srivastava, K. Das, Modeling of wire electro-discharge machining of TiC/Fe in situ metal matrix composite using normalized RBFN with enhanced k-means clustering technique, Int. J. Adv. Manuf. Technol. 43 (1–2) (2009) 107–116.

[32] A. Pramanik, A. Basak, Degradation of wire electrode during electrical discharge machining of metal matrix composites, Wear 346 (2016) 124–131.

https://doi.org/10.1016/j.heliyon.2019.e01473